Dark-Energy Dynamics Required to Solve the Cosmic Coincidence

Chas A. Egan
*Department of Astrophysics, School of Physics, University of New South Wales, Sydney, Australia**

Charles H. Lineweaver
Research School of Astronomy and Astrophysics, Australian National University, Canberra, Australia†

arXiv:0712.3099v1 [astro-ph] 19 Dec 2007

Dynamic dark energy (DDE) models are often designed to solve the cosmic coincidence (why, just now, is the dark energy density ρ_{de}, the same order of magnitude as the matter density ρ_m?) by guaranteeing $\rho_{de} \sim \rho_m$ for significant fractions of the age of the universe. This typically entails ad-hoc tracking or oscillatory behaviour in the model. However, such behaviour is neither sufficient nor necessary to solve the coincidence problem. What must be shown is that a significant fraction of observers see $\rho_{de} \sim \rho_m$. Precisely when, and for how long, must a DDE model have $\rho_{de} \sim \rho_m$ in order to solve the coincidence? We explore the coincidence problem in dynamic dark energy models using the temporal distribution of terrestrial-planet-bound observers. We find that any dark energy model fitting current observational constraints on ρ_{de} and the equation of state parameters w_0 and w_a, does have $\rho_{de} \sim \rho_m$ for a large fraction of observers in the universe. This demotivates DDE models specifically designed to solve the coincidence using long or repeated periods of $\rho_{de} \sim \rho_m$.

I. INTRODUCTION

In 1998, using supernovae Ia as standard candles, Riess et al. [1] and Perlmutter et al. [2] revealed a recent and continuing epoch of cosmic acceleration - strong evidence that Einstein's cosmological constant Λ, or something else with comparable negative pressure $p_{de} \sim -\rho_{de}$, currently dominates the energy density of the universe [3]. Λ is usually interpreted as the energy of zero-point quantum fluctuations in the vacuum [4, 5] with a constant equation of state $w \equiv p_{de}/\rho_{de} = -1$. This necessary additional energy component, construed as Λ or otherwise, has become generically known as "dark energy" (DE).

A plethora of observations have been used to constrain the free parameters of the new standard cosmological model, ΛCDM, in which Λ *does* play the role of the dark energy. Hinshaw et al. [6] find that the universe is expanding at a rate of $H_0 = 71 \pm 4\ km/s/Mpc$; that it is spatially flat and therefore critically dense ($\Omega_{tot0} = \frac{\rho_{tot0}}{\rho_{crit0}} = \frac{8\pi G}{3H_0^2}\rho_{tot0} = 1.01 \pm 0.01$); and that the total density is comprised of contributions from vacuum energy ($\Omega_{\Lambda 0} = 0.74 \pm 0.02$), cold dark matter (CDM; $\Omega_{CDM0} = 0.22 \pm 0.02$), baryonic matter ($\Omega_{b0} = 0.044 \pm 0.003$) and radiation ($\Omega_{r0} = 4.5 \pm 0.2 \times 10^{-5}$). Henceforth we will assume that the universe is flat ($\Omega_{tot0} = 1$) as predicted by inflation and supported by observations.

Two problems have been influential in moulding ideas about dark energy, specifically in driving interest in alternatives to ΛCDM. The first of these problems is concerned with the smallness of the dark energy density [4, 7, 8]. Despite representing more than 70% of the total energy of the universe, the current dark energy density is ~ 120 orders of magnitude smaller than energy scales at the end of inflation (or ~ 80 orders of magnitude smaller than energy scales at the end of inflation if this occurred at the GUT rather than Planck scale) [7]. Dark energy candidates are thus challenged to explain why the observed DE density is so small. The standard idea, that the dark energy is the energy of zero-point quantum fluctuations in the true vacuum, seems to offer no solution to this problem.

The second cosmological constant problem [9, 10, 11] is concerned with the near coincidence between the current cosmological matter density ($\rho_{m0} \approx 0.26 \times \rho_{crit0}$) and the dark energy density ($\rho_{de0} \approx 0.74 \times \rho_{crit0}$). In the standard ΛCDM model, the cosmological window during which these components have comparable density is short (just 1.5 e-folds of the cosmological scalefactor a) since matter density dilutes as $\rho_m \propto a^{-3}$ while vacuum density ρ_{de} is constant [12]. Thus, even if one explains why the DE density is much less than the Planck density (the smallness problem) one must explain why we happen to live during the time when $\rho_{de} \sim \rho_m$.

To quantify the time-dependent proximity of ρ_m and ρ_{de}, we define a proximity parameter,

$$r \equiv \min\left[\frac{\rho_{de}}{\rho_m}, \frac{\rho_m}{\rho_{de}}\right], \tag{1}$$

which ranges from $r \approx 0$, when many orders of magnitude separate the two densities, to $r = 1$, when the two densities are equal. The presently observed value of this parameter is $r_0 = \frac{\rho_{m0}}{\rho_{de0}} \approx 0.35$. In terms of r, the coincidence problem is as follows. If we naively presume that the time of our observation t_{obs} has been drawn from a distribution of times $P_t(t)$ spanning many decades of cosmic scalefactor, we find that the expected proximity parameter is $r \approx 0 \ll 0.35$. In the top panel of Fig. 1 we

*Visiting the Research School of Astronomy and Astrophysics, Australian National University; Electronic address: chas@mso.anu.edu.au
†Planetary Science Institute, Australian National University; Research School of Earth Sciences, Australian National University

use a naive distribution for t_{obs} that is constant in $\log(a)$ to illustrate how observing r as large as $r_0 \approx 0.35$ seems unexpected.

In Lineweaver and Egan [12] we showed how the apparent severity of the coincidence problem strongly depends upon the distribution $P_t(t)$ from which t_{obs} is hypothesized to have been drawn. Naive priors for t_{obs}, such as the one illustrated in the top panel of Fig. 1, lead to naive conclusions. However, the coincidence problem can be more meaningfully quantified when the necessary constraint that t_{obs} has been drawn from the temporal distribution of observers is included. The temporal and spatial distribution of observers has been estimated using large ($10^{11} M_{\odot}$) galaxies [13, 14, 15] and terrestrial planets [12] as tracers. The top panel of Fig. 1 shows the temporal distribution of observers $P_t(t)$ from Lineweaver and Egan [12].

In Lineweaver and Egan [12] we assessed the severity of the coincidence problem under ΛCDM. We showed that our observed proximity $r \approx 0.35$ is a typical observation for terrestrial-planet bound observers. This result follows directly from the approximate alignment of the $P_t(t)$ and $r(t)$ peaks in the top panel of Fig. 1.

The smallness of the dark energy density has been anthropically explained in multiverse models with the argument that in universes with much larger DE components, DE driven acceleration starts earlier and precludes the formation of galaxies and large scale structure. Such universes are probably devoid of observers [14, 16, 17]. A solution to the coincidence problem in this scenario was outlined by Garriga et al. [15] who showed that if ρ_{de} is low enough to allow galaxies to form, then observers in those galaxies will observe $r \sim 1$.

Another possible extension of the concordance cosmological model that may explain the observed smallness of ρ_{de} is the generalization of dark energy candidates to include dynamic dark energy (DDE) models such as quintessence, phantom dark energy, k-essence and Chaplygin gas. In these models the dark energy is treated as a new matter field which is approximately homogenous, and evolves as the universe expands. DDE evolution offers a mechanism for the decay of ρ_{de} from the expected Planck scales (10^{93} g/cm^3) in the early universe (10^{-44} s) to the small value we observe today (10^{-30} g/cm^3). The light grey shade in the bottom panel of Fig. 1 represents contemporary observational constraints on the DDE density history. Many DDE models are designed to solve the coincidence problem by having $\rho_{de} \sim \rho_m$ for a large fraction of the history/future of the universe [18, 19, 20, 21, 22, 23, 24, 25, 26, 27, 28, 29, 30, 31, 32, 33, 34, 35, 36, 37, 38, 39, 40, 41]. With $\rho_{de} \sim \rho_m$ for extended or repeated periods the hope is to ensure that $r \sim 1$ is expected.

Our main goal in this paper is to take into account the temporal distribution of observers to determine when, and for how long, a DDE model must have $\rho_{de} \sim \rho_m$ in order to solve the coincidence problem? Specifically, we extend the work of Lineweaver and Egan [12] to find

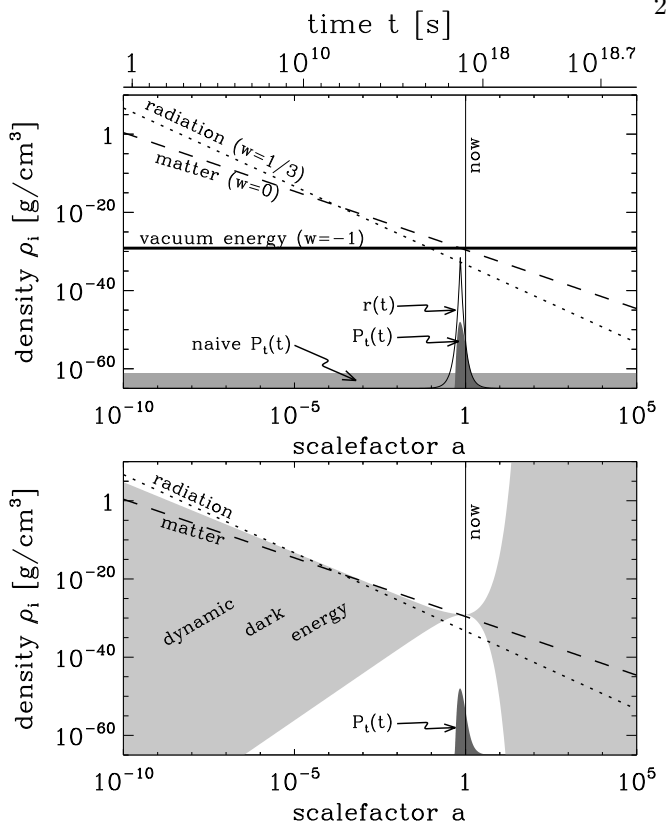

FIG. 1: **(Top)** The history of the energy density of the universe according to standard ΛCDM. The dotted line shows the energy density in radiation (photons, neutrinos and other relativistic modes). The radiation density dilutes as a^{-4} as the universe expands. The dashed line shows the density in ordinary non-relativistic matter, which dilutes as a^{-3}. The thick solid line shows the energy of the vacuum (the cosmological constant) which has remained constant since the end of inflation. The thin solid peaked curve shows the proximity r of the matter density to the vacuum energy density (see Eq. 1). The proximity r is only ~ 1 for a brief period in the $log(a)$ history of the cosmos. Whether or not there is a coincidence problem depends on the distribution $P_t(t)$ for t_{obs}. If one naively assumes that we could have observed any epoch with equal probability (the light grey shade) then we should not expect to observe r as large as we do. If, however, $P_t(t)$ is based on an estimate of the temporal distribution of observers (the dark grey shade) then $r_0 \approx 0.35$ is not surprising, and the coincidence problem is solved under ΛCDM [12]. **(Bottom)** The dark energy density history is modified in DDE models. Observational constraints on the dark energy density history are represented by the light grey shade (details in Section III).

out for which cosmologies (in addition to ΛCDM) the coincidence problem is solved when the temporal distribution of observers is considered. In doing this we answer the question, Does a dark energy model fitting contemporary constraints on the density ρ_{de} and the equation of state parameters, necessarily solve the cosmic coincidence? Both positive and negative answers have interesting consequences. An answer in the affirmative will simplify considerations that go into DDE modeling: the coincidence is solved by all models fitting cosmological

constraints. An answer in the negative would yield a new opportunity to constrain the DE equation of state parameters *more strongly* than contemporary cosmological surveys.

A different coincidence problem arises when the time of observation is conditioned on and the parameters of a model are allowed to slide. The tuning of parameters and the necessity to include ad-hoc physics are large problems for many current dark energy models. This paper does not address such issues, and the interested reader is referred to Hebecker and Wetterich [42], Bludman [43] and Linder [44]. The coincidence problem addressed here is when the observation of $r \geq 0.35$ is unlikely according to the model [9, 10, 11].

In Section II we present several examples of DDE models used to solve the coincidence problem. An overview of observational constraints on DDE is given in Section III. In Section IV we estimate the temporal distribution of observers. Our main analysis is presented in Section V. Our main result - that the coincidence problem is solved for all DDE models fitting observational constraints - is illustrated in Fig. 7. Finally, in Section VI, we end with a discussion of our results, their implications and potential caveats.

II. DYNAMIC DARK ENERGY MODELS IN THE FACE OF THE COSMIC COINCIDENCE

Though it is beyond the scope of this article to provide a complete review of DDE (see Copeland et al. [45], Szydłowski et al. [46]), here we give a few representative examples in order to set the context and motivation of our work. Fig. 2 illustrates density histories typical of tracker quintessence, tracking oscillating energy, interacting quintessence, phantom dark energy, k-essence, and Chaplygin gas. They are discussed in turn below.

A. Quintessence

In quintessence models the dark energy is interpreted as a homogenous scalar field with Lagrangian density $\mathcal{L}(\phi, X) = \frac{1}{2}\dot{\phi}^2 - V(\phi)$ [47, 48, 49, 50, 51, 52, 53]. The evolution of the quintessence field and of the cosmos depends on the postulated potential $V(\phi)$ of the field and on any postulated interactions. In general, quintessence has a time-varying equation of state $w = \frac{p_{de}}{\rho_{de}} = \frac{\dot{\phi}^2/2 - V(\phi)}{\dot{\phi}^2/2 + V(\phi)}$. Since the kinetic term $\dot{\phi}^2/2$ cannot be negative, the equation of state is restricted to values $w \geq -1$. Moreover, if the potential $V(\phi)$ is non-negative then w is also restricted to values $w \leq +1$.

If the quintessence field only interacts gravitationally then energy density evolves as $\frac{\delta\rho_{de}}{\rho_{de}} = -3(w+1)\frac{\delta a}{a}$ and the restrictions $-1 \leq w \leq +1$ mean ρ_{de} decays (but never faster than a^{-6}) or remains constant (but never increases).

1. Tracker Quintessence

Particular choices for $V(\phi)$ lead to interesting attractor solutions which can be exploited to make ρ_{de} scale ("track") sub-dominantly with $\rho_r + \rho_m$.

The DE can be forced to transit to a Λ-like ($w \approx -1$) state at any time by fine-tuning $V(\phi)$. In the Λ-like state ρ_{de} overtakes ρ_m and dominates the recent and future energy density of the universe. We illustrate tracker quintessence in Fig. 2 using a power law potential $V(\phi) = M\phi^{-\alpha}$ (panel b) [48, 50, 52] and an exponential potential $V(\phi) = M\exp(1/\phi)$ (panel c) [19].

The tracker paths are attractor solutions of the equations governing the evolution of the field. If the tracker quintessence field is initially endowed with a density off the tracker path (e.g. an equipartition of the energy available at reheating) its density quickly approaches and joins the tracker solution.

2. Oscillating Dark Energy

Dodelson et al. [19] explored a quintessence potential with oscillatory perturbations $V(\phi) = M\exp(-\lambda\phi)\,[1 + A\sin(\nu\phi)]$. They refer to models of this type as tracking oscillating energy. Without the perturbations (setting $A = 0$) this potential causes exact tracker behaviour: the quintessence energy decays as $\rho_r + \rho_m$ and never dominates. With the perturbations the quintessence energy density oscillates about $\rho_r + \rho_m$ as it decays (Fig. 2d). The quintessence energy dominates on multiple occasions and its equation of state varies continuously between positive and negative values. One of the main motivations for tracking oscillating energy is to solve the coincidence problem by ensuring that $\rho_{de} \sim \rho_m$ or $\rho_{de} \sim \rho_r$ at many times in the past or future.

It has yet to be seen how such a potential might arise from particle physics. Phenomenologically similar cosmologies have been discussed in Ahmed et al. [25], Feng et al. [36], Yang and Wang [54].

3. Interacting Quintessence

Non-gravitational interactions between the quintessence field and matter fields might allow energy to transfer between these components. Such interactions are not forbidden by any known symmetry [55]. The primary motivation for the exploration of interacting dark energy models is to solve the coincidence problem. In these models the present matter/dark energy density proximity r may be constant [18, 22, 26, 29, 30, 31, 33, 35, 38, 39, 40, 56] or slowly varying [28, 34].

We plot a density history of the interacting quintessence model of Amendola [18] in Fig. 2e. This model is characterized by a DE potential $V(\phi) =$

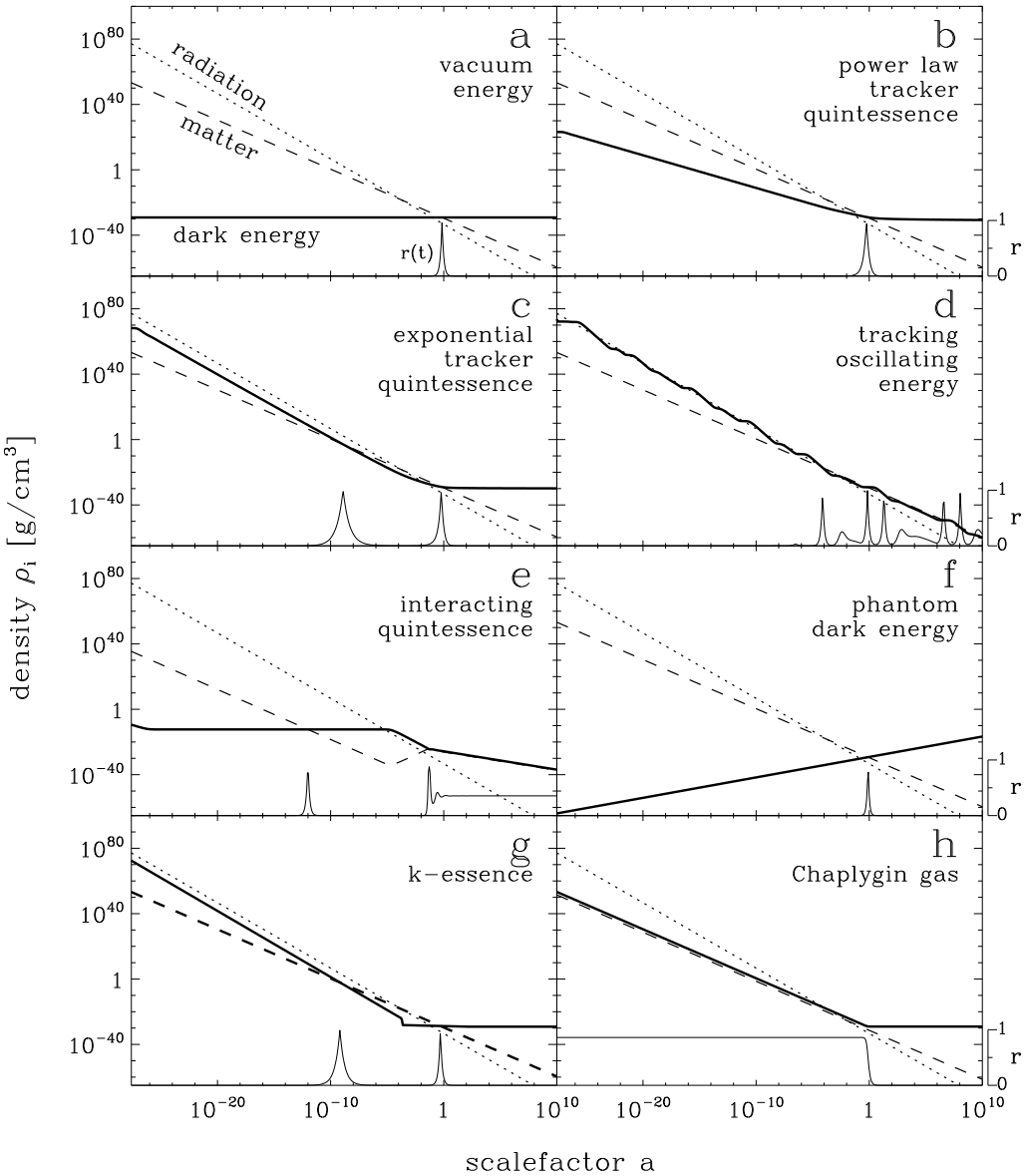

FIG. 2: The energy density history of the universe according to ΛCDM (panel a), and seven DDE models selected from the literature (see text for references). In each panel the radiation and matter densities are the dotted and dashed lines respectively. The DE density is given by the thick black line. The proximity parameter r is given by the thin black line at the base of each panel. Of the DDE models shown here, tracker quintessence and k-essence (panels b, c and g) have $r \sim 1$ for a small fraction of the life of the universe (whether the abscissa is t, $\log(t)$, a, $\log(a)$, or any other of a large number of measures). On the other hand, tracking oscillating energy, interacting quintessence, phantom DE and Chaplygin gas (panels d, e, f and h) exhibit $r \sim 1$ for a large fraction of the life of the universe. For the phantom DE example (panel f) this is true in t, but not in a or $\log(a)$. In phantom models the future universe grows super-exponentially to $a = \infty$ (a "big-rip") shortly after matter-DE equality. Thus the universe spends a large fraction of *time* with $r \sim 1$, however this is is not seen in $\log(a)$-space. For each of the models in this figure, numerical values for free parameters were chosen to crudely fit observational constraints and are given in Appendix A.

$A\exp[B\phi]$ and DE-matter interaction term $Q = -C\rho_m\dot{\phi}$, specifying the rate at which energy is transferred to the matter fields. The free parameters were tuned such that radiation domination ends at $a = 10^{-5}$ and that $r_{t\to\infty} = 0.35$.

B. Phantom Dark Energy

The analyses of Riess et al. [57] and Wood-Vasey et al. [58] have mildly ($\sim 1\sigma$) favored a dark energy equation of state $w_{de} < -1$. These values are unattainable by stan-

dard quintessence models but can occur in phantom dark energy models [59], in which kinetic energies are negative. The energy density in the phantom field *increases* with scalefactor, typically leading to a future "big rip" singularity where the scalefactor becomes infinite in finite time. Fig. 2f shows the density history of a simple phantom model with a constant equation of state $w = -1.25$. The big rip ($a = \infty$ at $t = 57.5$ Gyrs) is not seen in $\log(a)$-space.

Caldwell et al. [60] and Scherrer [32] have explored how phantom models may solve the coincidence problem: since the big rip is triggered by the onset of DE domination, such cosmologies spend a significant fraction of their total time with r large. For the phantom model with $w = -1.25$ (Fig. 2f) Scherrer [32] finds $r > 0.1$ for 12% of the total lifetime of the universe. Whether this solves the coincidence or not depends upon the prior probability distribution $P_t(t)$ for the time of observation. Caldwell et al. [60] and Scherrer [32] implicitly assume that the temporal distribution of observers is constant in time (i.e. $P_t(t) = \text{constant}$). For this prior the coincidence problem *is* solved because the chance of observing $r \geq 0.1$ is large (12%). Note that for the "naive $P_t(t)$" prior shown in Fig. 1, the solution of Caldwell et al. [60] and Scherrer [32] fails because $r > 0.1$ is brief in $\log(a)$-space. It fails in this way for many other choices of $P_t(t)$ including, for example, distributions constant in a or $\log(t)$.

C. K-Essence

In k-essence the DE is modeled as a scalar field with non-canonical kinetic energy [61, 62, 63, 64]. Non-canonical kinetic terms can arise in the effective action of fields in string and supergravity theories. Fig. 2g shows a density history typical of k-essence models. This particular model is from Armendariz-Picon et al. [63] and Steinhardt [10]. During radiation domination the k-essence field tracks radiation sub-dominantly (with $w_{de} = w_r = 1/3$) as do some of the other models in Fig. 2. However, no stable tracker solution exists for $w_{de} = w_m (= 0)$. Thus after radiation-matter equality, the field is unable to continue tracking the dominant component, and is driven to another attractor solution (which is generically Λ-like with $w_{de} \approx -1$). The onset of DE domination was recent in k-essence models because matter-radiation equality prompts the transition to a Λ-like state. K-essence thereby avoids fine-tuning in any particular numerical parameters, but the Lagrangian has been constructed ad-hoc.

D. Chaplygin Gas

A special fluid known as Chaplygin gas motivated by braneworld cosmology may be able to play the role of dark matter *and* the dark energy [65, 66]. Generalized Chaplygin gas has the equation of state $p_{de} = -A\rho_{de}^{-\alpha}$ which behaves like pressureless dark matter at early times ($w_{de} \approx 0$ when ρ_{de} is large), and like vacuum energy at late times ($w_{de} \approx -1$ when ρ_{de} is small). In Fig. 2h we show an example with $\alpha = 1$.

E. Summary of DDE Models

Two broad classes of DDE models emerge from our comparison:

1. In ΛCDM, tracker quintessence and k-essence models, the dark energy density is vastly different from the matter density for most of the lifetime of the universe (panels a, b, c, g of Fig. 2). The coincidence problem can only be solved if the probability distribution $P_t(t)$ for the time of observation is narrow, and overlaps significantly with an $r \sim 1$ peak. If $P_t(t)$ is wide, e.g. constant over the life of the universe in t or $\log(t)$, then observing $r \sim 1$ would be unlikely in these models and the coincidence problem *is not* resolved.

2. Tracking oscillating energy, interacting quintessence, phantom models and Chaplygin gas models (panels d, e, f, h of Fig. 2) employ mechanisms to ensure that $r \sim 1$ for large fractions of the life of the universe. In these models the coincidence problem may be solved for a wider range of $P_t(t)$ including, depending on the DE model, distributions that are constant over the whole life of the universe in t, $\log(t)$, a or $\log(a)$.

The importance of an estimate of the distribution $P_t(t)$ is highlighted: such an estimate will either rule out models of the first category because they do not solve the coincidence problem, or demotivate models of the second because their mechanisms are unnecessary to solve the coincidence problem.

We leave this line of enquiry temporarily to discuss contemporary *observational* constraints on the dark energy density history, because we wish to test what DE dynamics are required to solve the coincidence, beyond those which models must exhibit to satisfy standard cosmological observations.

III. CURRENT OBSERVATIONAL CONSTRAINTS ON DYNAMIC DARK ENERGY

A. Supernovae Ia

Observationally, possible dark energy dynamics is explored almost solely using measurements of the cosmic expansion history. Recent cosmic expansion is directly probed by using type Ia supernova (SNIa) as standard candles [1, 2]. Each observed SNIa provides an independent measurement of the luminosity distance d_l to the

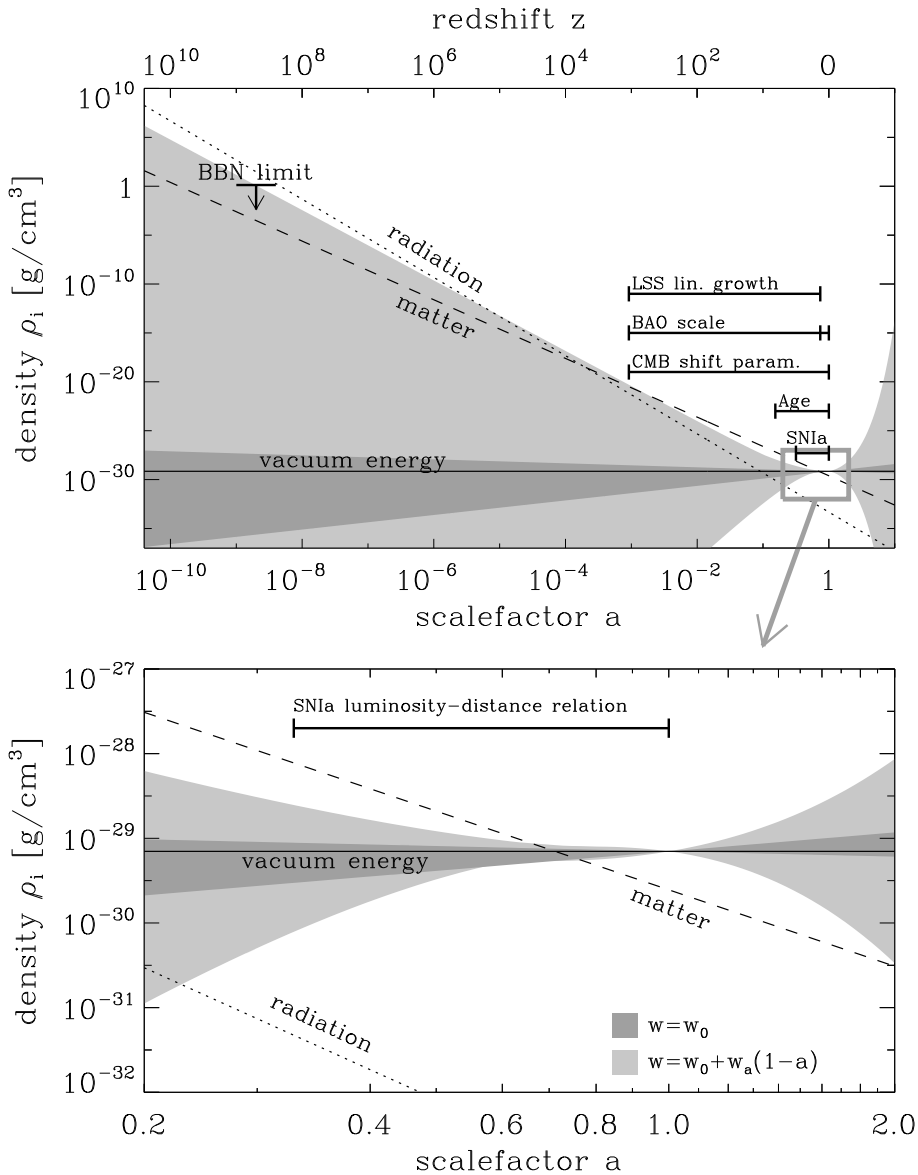

FIG. 3: The energy densities of radiation ρ_r, matter ρ_m and the cosmological constant ρ_Λ are shown as a function of scalefactor, by the dotted, dashed, and solid lines respectively. Cosmological probes of dark energy include SNIa, CMB, BAO, the LSS linear growth factor and constraints from BBN (see text). Each of these probes is sensitive to the effects of dark energy over different redshift intervals, as indicated. The light grey band envelopes w_0-w_a-parameterized DDE models allowed at $< 2\sigma$ by Davis et al. [67] (the contour in $w_0 - w_a$ space is shown explicitly in Fig. 7). The dark grey band envelopes w_0-parameterized DDE models ($w_a = 0$ assumed) allowed at $< 2\sigma$ by Wood-Vasey et al. [58]. The constraint is $w = -1.09 \pm 0.16$ at 2σ.

redshift of the supernova z_{SN}. The luminosity distance to z_{SN} is given by

$$d_l(z_{SN}) = (1 + z_{SN})\frac{c}{H_0}\int_{z=0}^{z_{SN}} \frac{dz}{E(z)} \qquad (2)$$

where

$$E(z) \;=\; \frac{H(z)}{H_0} \qquad (3)$$

$$= \left[\Omega_{r0}(1+z)^4 + \Omega_{m0}(1+z)^3 + \Omega_{de0}\frac{\rho_{de}(z)}{\rho_{de0}}\right]^{\frac{1}{2}}$$

and thus depends on H_0, Ω_{m0}, and the evolution of the dark energy $\rho_{de}(z)/\rho_{de0}$. The radiation term, irrelevant at low redshifts, can be dropped from Equation 3. Ω_{de0} is a dependent parameter due to flatness ($\Omega_{de0} = 1 - \Omega_{m0}$). Contemporary datasets include ~ 200 supernovae at redshifts $z_{SN} \leq 2.16$ ($a \geq 0.316$) [58, 68] and provide an effective continuum of constraints on the expansion his-

tory over that range [69, 70]. The redshift range probed by SNIa is indicated in both panels of Fig. 3.

B. Cosmic Microwave Background

The first peak in the cosmic microwave background (CMB) temperature power spectrum corresponds to density fluctuations on the scale of the sound horizon at the time of recombination. Subsequent peaks correspond to higher-frequency harmonics. The locations of these peaks in l-space depend on the comoving scale of the sound horizon at recombination, and the angular distance to recombination. This is summarized by the so-called CMB shift parameter R [71, 72] which is related to the cosmology by

$$R = \sqrt{\Omega_{m0}} \int_{z=0}^{z_{rec}} \frac{dz}{E(z)} \tag{4}$$

where $z_{rec} \approx 1089$ [73] is the redshift of recombination. The 3-year WMAP data gives a shift parameter $R = 1.71 \pm 0.03$ [67, 73]. Since the dependence of Equation 4 on H_0 and Ω_{m0} differs from that of Equation 2, measurements of the CMB shift parameter can be used to break degeneracies between H_0, Ω_{m0} and DE evolution in the analysis of SNIa. In the top panel of Fig. 3 we represent the CMB observations using a bar from $z = 0$ to z_{rec}.

C. Baryonic Acoustic Oscillations and Large Scale Structure

As they imprinted acoustic peaks in the CMB, the baryonic oscillations at recombination were expected to leave signature wiggles - baryonic acoustic oscillations (BAO) - in the power spectrum of galaxies [74]. These were detected with significant confidence in the SDSS luminous red galaxy power spectrum [75]. The expected BAO scale depends on the scale of the sound horizon at recombination, and on transverse and radial scales at the mean redshift z_{BAO}, of galaxies in the survey. Eisenstein et al. [75] measured the quantity

$$A(z_{BAO}) = \frac{\sqrt{\Omega_{m0}}}{E(z_{BAO})^{\frac{1}{3}}} \left[\frac{1}{z_{BAO}} \int_{z=0}^{z_{BAO}} \frac{dz}{E(z)} \right]^{\frac{2}{3}} \tag{5}$$

to have a value $A(z_{BAO} = 0.35) = 0.469 \pm 0.017$, thus constraining the matter density and the dark energy evolution parameters in a configuration which is complomentary to the CMB shift parameter and the SNIa luminosity distance relation. Ongoing BAO projects have been designed specifically to produce stronger constraints on the dark energy equation of state parameter w. For example, WIGGLEZ [76] will use a sample of high-redshift galaxies to measure the BAO scale at $z_{BAO} \approx 0.75$. As well as reducing the effects of non-linear clustering, this redshift is at a larger angular distance, making the observed scale more sensitive to w. Constraints from the BAO scale depend on the evolution of the universe from z_{rec} to z_{BAO} to set the physical scale of the oscillations. They also depend on the evolution of the universe from z_{BAO} to $z = 0$, since the observed angular extent of the oscillations depends on this evolution. The bar representing BAO scale observations in the top panel of Fig. 3 indicates both these regimes.

The amplitude of the BAOs - the amplitude of the large scale structure (LSS) power spectrum - is determined by the amplitude of the power spectrum at recombination, and how much those fluctuations have grown (the transfer function) between z_{rec} and z_{BAO}. By comparing the recombination power spectrum (from CMB) with the galaxy power spectrum, the LSS linear growth factor can be measured and used to constrain the expansion history of the universe (independently of the BAO scale) over this redshift range. In practice, biases hinder precise normalization of the galaxy power spectrum, weakening this technique. The range over which this technique probes the DE is indicated in Fig. 3.

D. Ages

Cosmological parameters from SN1a, CMB, LSS, BAO and other probes allow us to calculate the current age of the universe to be 13.8 ± 0.1 [6] assuming ΛCDM. Uncertainties on the age calculated in this way grow dramatically if we drop the assumption that the DE is vacuum energy ($w = -1$).

An independent lower limit on the current age of the universe is found by estimating the ages of the oldest known globular clusters [77]. These observations rule out models which predict the universe to be younger than 12.7 ± 0.7 Gyrs (2σ confidence):

$$\begin{aligned} t_0 &= H_0^{-1} \int_{z=0}^{\infty} \frac{dz}{(1+z)E(z)} \\ &\gtrsim 12.7 \pm 0.7 \text{ Gyrs.} \end{aligned} \tag{6}$$

Other objects can also be used to set this age limit Lineweaver [78], but generally less successfully due to uncertainties in dating techniques.

Assuming ΛCDM, an age of 12.7 Gyrs corresponds to a redshift of $z \approx 5.5$. Contemporary age measurements are sensitive to the dark energy content from $z \approx 5.5$ to $z = 0$. In the top panel of Fig. 3 we show this redshift interval. The evolution and energy content of the universe before 12.7 Gyrs ago is not probed by these age constraints.

E. Nucleosynthesis

In addition to the constraints on the expansion history (SN1a, CMB, BAO and t_0) we know that $\rho_{de}/\rho_{tot} < 0.045$ (at 2σ confidence) during Big Bang Nucleosynthesis

(BBN) [79]. Larger dark energy densities imply a higher expansion rate at that epoch ($z \sim 6 \times 10^8$) which would result in a lower neutron to proton ratio, conflicting with the measured helium abundance, $Y_{\rm He}$.

F. Dark Energy Parameterization

Because of the variety of proposed dark energy models, it has become usual to summarize observations by constraining a parameterized time-varying equation of state. Dark energy models are then confronted with observations in this parameter space. The unique zeroth order parameterization of w is $w = w_0$ (a constant), with $w = -1$ characterizing the cosmological constant model. The observational data can be used to constrain the first derivative of w. This additional dimension in the DE parameter space may be useful in distinguishing models which have the same w_0. From an observational standpoint, the obvious choice of 1st order parameterization is $w(z) = w_0 + \frac{dw}{dz} z$ [80]. This is rarely used today since currently considered DDE models are poorly portrayed by this functional form. The most popular parameterization is $w(a) = w_0 + w_a(1-a)$ [81, 82], which does not diverge at high redshift.

Linder and Huterer [83] have argued that the extension of this approach to second order, e.g. $w(a) = w_0 + w_a(1-a) + w_{aa}(1-a)^2$, is not motivated by current DDE models. Moreover, they have shown that next generation observations are unlikely to be able to distinguish the quadratic from a linear expansion of w. Riess et al. [68] have illustrated this recently using new SN1a.

An alternative technique for exploring the history of dark energy is to constrain $w(z)$ or $\rho_{de}(z)$ in independent redshift bins. This technique makes fewer assumptions about the specific shape of $w(z)$. In the absence of any strongly motivated parameterization of $w(z)$ this bin-wise method serves as a good reminder of how little we actually know from observation. Using luminosity distance measurements from SNIa, DE evolution has been constrained in this way in $\Delta z \sim 0.5$ bins out to redshift $z_{SN} \sim 2$ [68, 84, 85]. In the future, BAO measurements at various redshifts may contribute to these constraints, however z_{BAO} will probably never be larger than z_{SN}. Moreover, because the recombination redshift $z_{rec} \approx 1089$ is fixed, only the cumulative effect (from $z = z_{rec}$ to $z = 0$) of the DE can be measured with the CMB and LSS linear growth factor. With only this single data point above z_{SN}, the bin-wise technique effectively degenerates to a parameterized analysis at $z > z_{SN}$.

G. Summary of Current DDE Constraints

If one assumes the popular $w_0 - w_a$ parameterization until last scattering, then all cosmological probes can be combined to constrain w_0 and w_a. In a recent analysis of SN1a, CMB and BAO observations, Davis et al. [67] found $w_0 = -1.0 \pm 0.4$ and $w_a = -0.4 \pm 1.8$ at 2σ confidence (the contour is shown in Fig. 7). Using the same observations, Wood-Vasey et al. [58] assumed $w_a = 0$ and found $w = w_0 = -1.09 \pm 0.16$ (2σ).

The evolution of ρ_{de} is related to w by covariant energy conservation [86]

$$\frac{\delta \rho_{de}}{\rho_{de}} = -3\,(w(a)+1)\,\frac{\delta a}{a}. \tag{7}$$

The dark energy density corresponding to the $w_0 - w_a$ parameterization of w is thus given by

$$\rho_{de}(z) = \rho_{de0}\; e^{3w_a(a-1)}\; a^{-3(1+w_0+w_a)}. \tag{8}$$

The cosmic energy density history is illustrated in Fig. 3. Radiation and matter densities steadily decline as the dotted and dashed lines. With the DE equation of state parameterized as $w(a) = w_0 + w_a(1-a)$, its density history is constrained to the light-grey area [67]. If the evolution of w is negligible, i.e. we condition on $w_a \approx 0$, then $w(a) \approx w_0$ and the DE density history lies within the dark-grey band [58]. If the dark energy is pure vacuum energy (or Einstein's cosmological constant) then $w = -1$ and its density history is given by the horizontal solid black line.

IV. THE TEMPORAL DISTRIBUTION OF OBSERVERS

The energy densities ρ_r, ρ_m and ρ_{de}, and the proximity parameter r we imagine we might have observed, depend on the distribution $P_t(t)$ from which we imagine our time of observation t_{obs} has been drawn. What we can expect to observe must be restricted by the conditions necessary for our presence as observers [87]. Thus, for example, it is meaningless to suppose we might have lived during inflation, or during radiation domination, or before the first atoms [88].

We can, however, suppose that we are randomly selected cosmology-discovering observers, and we can expect our observations of ρ_m and ρ_{de} to be typical of observations made by such observers. This is Vilenkin's principle of mediocrity [89]. Accordingly, the distribution $P_t(t)$ for the time of observation t_{obs} is proportional to the temporal distribution of cosmology-discovering observers (referred to henceforth as simply "observers"). Thus to solve the coincidence problem one must show that the proximity parameter we measure, r_0, is typical of those measured by other observers.

The most abundant elements in the cosmos are hydrogen, helium, oxygen and carbon [90]. In the past decade > 200 extra solar planets have been observed via doppler, transit or microlensing methods. Extrapolation of current patterns in planet mass and orbital period are consistent with the idea that planetary systems like our own are common in the universe [91]. All this does not necessarily imply that observers are common, but it does support the idea that terrestrial-planet-bound carbon-based

observers, even if rare, may be the *most common* observers. In the following estimation of $P_t(t)$ we consider only observers bound to terrestrial planets.

A. First the Planets...

Lineweaver [92] estimated the terrestrial planet formation rate (PFR) by making a compilation of measurements of the cosmic star formation rate (SFR) and suppressing a fraction of the early stars $f(t)$ to correct for the fact that the metallicity was too low for those early stars to host terrestrial planetary systems,

$$PFR(t) = const \times SFR(t) \times f(t). \quad (9)$$

In Fig. 4 we plot the PFR reported by Lineweaver [92] as a function of redshift, $z = \frac{1}{a} - 1$. As illustrated in the figure, there is large uncertainty in the normalization of the formation history. Our analysis will not depend on the normalization of this function so this uncertainty *will not* propagate into our analysis. There are also uncertainties in the location of the turnover at high redshift, and in the slope of the formation history at low redshift - both of these *will* affect our results.

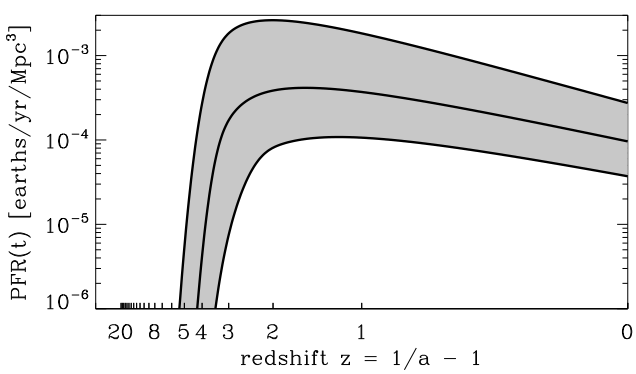

FIG. 4: The terrestrial planet formation rate as estimated by Lineweaver [92]. It is based on a compilation of SFR measurements and has been corrected for the low metallicity of the early universe, which prevents the terrestrial planet formation rate from rising as quickly as the stellar formation rate at $z \gtrsim 4$.

The conversion from redshift to time depends on the particular cosmology, through the Friedmann equation,

$$\begin{aligned} \left(\frac{da}{dt}\right)^2 &= H(a)^2 a^2 \quad (10) \\ &= H_0^2 \Big[\Omega_{r0} a^{-2} + \Omega_{m0} a^{-1} + \\ &\quad \Omega_{de0} \ \exp[3w_a(a-1)] \ a^{-3w_0 - 3w_a - 1} \Big]. \end{aligned}$$

In Fig. 5 we plot the PFR from Fig. 4 as a function of time assuming the best fit parameterized DDE cosmology.

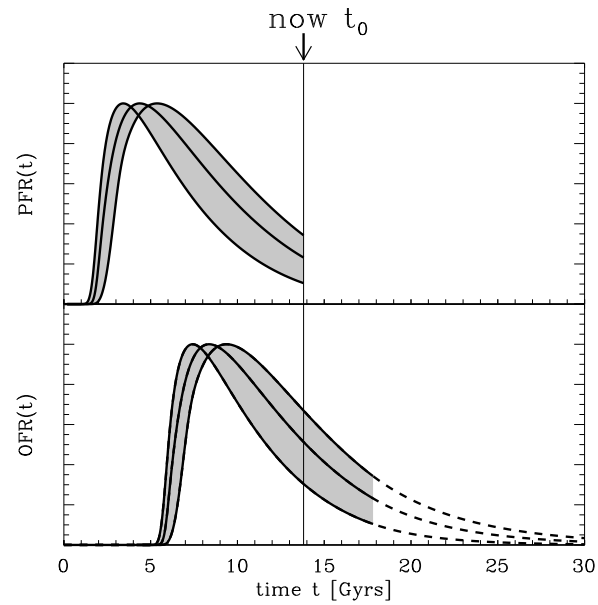

FIG. 5: The terrestrial planet formation from Fig. 4 is shown here as a function of time. The transformation from redshift to time is cosmology dependent. To create this figure we have used best-fit values for the DDE parameters, $w_0 = -1.0$ and $w_a = -0.4$ [67]. The y-axis is linear (c.f. the logarithmic axis in Fig. 4) and the family of curves have been renormalized to highlight the sources of uncertainty important for this analysis: uncertainty in the width of the function, and in the location of its peak. The observer formation rate (OFR) is calculated by shifting the planet formation rate by some amount Δt_{obs} (= 4 Gyrs) to allow the planet to cool, and the possible emergence of observers. These distributions are closed by extrapolating exponentially in t.

B. ... then First Observers

After a star has formed, some non-trivial amount of time Δt_{obs} will pass before observers, if they arise at all, arise on an orbiting rocky planet. This time allows planets to form and cool and, possibly, biogenesis and the emergence observers. Δt_{obs} is constrained to be shorter than the life of the host star. If we consider that our Δt_{obs} has been drawn from a probability distribution $P_{\Delta t_{obs}}(t)$. The observer formation rate (OFR) would then be given by the convolution

$$OFR(t) = const \times \int_0^\infty PFR(\tau) P_{\Delta t_{obs}}(t - \tau) d\tau. \quad (11)$$

In practice we know very little about $P_{\Delta t_{obs}}(t)$. It must be very nearly zero below about $\Delta t_{obs} \sim 0.5$ Gyrs - this is the amount of time it takes for terrestrial planets to cool and the bombardment rate to slow down. Also, it must be near zero above the lifetime of a small ($0.1 M_\odot$) star (above $\sim$ 500 Gyrs). If we assume that our Δt_{obs} is typical, then $P_{\Delta t_{obs}}(t)$ has significant weight around $\Delta t_{obs} = 4$ Gyrs - the amount of time it has taken for us to evolve here on Earth.

A fiducial choice, where *all* observers emerge 4 Gyrs after the formation of their host planet, is $P_{\Delta t_{obs}}(t) = \delta(t-4\text{ Gyrs})$. This choice results in an OFR whose shape is the same as the PFR, but is shifted 4 Gyrs into the future,

$$OFR(t) = const \times PFR(t - 4\text{ Gyrs}) \tag{12}$$

(see the lower panel of Fig. 5). Even for non-standard w_0 and w_a values, this fiducial OFR aligns closely with the $r(t)$ peak and the effect of a wider $P_{\Delta t_{obs}}$ is generally to increase the severity of the coincidence problem by spreading observers outside the $r(t)$ peak. Hence using our fiducial $P_{\Delta t_{obs}}$ (which is the narrowest possibility) will lead to conclusions which are conservative in that they underestimate the severity of the cosmic coincidence. If another choice for $P_{\Delta t_{obs}}$ could be justified, the cosmic coincidence would be more severe than estimated here. We will discuss this choice in Section VI.

The OFR is then extrapolated into the future using a decaying exponential with respect to t (the dashed segment in the lower panel of Fig. 5). The observed SFH is consistent with a decaying exponential. We have tested other choices (linear & polynomial decay) and our results do not depend strongly on the shape of the extrapolating function used.

The temporal distribution of observers $P_t(t)$ is proportional to the observer formation rate,

$$P_t(t) = const \times OFR(t). \tag{13}$$

This observer distribution is similar to the one used by Garriga et al. [15] to treat the coincidence problem in a multiverse scenario. By comparison, our $OFR(t)$ distribution starts later because we have considered the time required for the build up of metallicity, and because we have included an evolution stage of 4 Gyrs. Our distribution also decays more quickly than theirs does. Some of our cosmologies suffer big-rip singularities in the future. In these cases we truncate $P_t(t)$ at the big-rip.

V. ANALYSIS AND RESULTS: DOES FITTING CONTEMPORARY CONSTRAINTS NECESSARILY SOLVE THE COSMIC COINCIDENCE?

For a given model the proximity parameter observed by a typical observer is described by a probability distribution $P_r(r)$ calculated as

$$P_r(r) = \sum \frac{dt}{dr} P_t(t(r)). \tag{14}$$

The summation is over contributions from all solutions of $t(r)$ (typically, any given value of r occurs at multiple times during the lifetime of the Universe). In Fig. 6 we plot $P_r(r)$ for the $w_0 = -1.0$, $w_a = -0.4$ cosmology. In this case, observers are distributed over a wide range of r values, with 71% seeing $r > r_0$, and 29% seeing $r < r_0$.

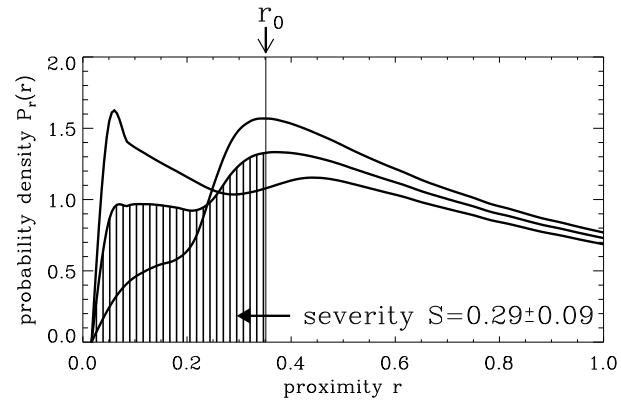

FIG. 6: The predicted distribution of observations of r is plotted for the parameterized DDE model which best-fits cosmological observations: $w_0 = -1.0$ and $w_a = -0.4$. The proximity parameter we observe $r_0 = \frac{\rho_{m0}}{\rho_{de0}} \approx 0.35$ is typical in this cosmology since only 29% of observers (vertical striped area) observe $r < 0.35$. The upper and lower limits on this value resulting from uncertainties in the SFR are 38% and 20% respectively. Thus the severity of the cosmic coincidence in this model is $S = 0.29 \pm 0.09$. This model does not suffer a coincidence problem.

We define the severity S of the cosmic coincidence problem as the probability that a randomly selected observer measures a proximity parameter r lower than we do:

$$S = P(r < r_0) = 1 - P(r > r_0) = \int_{r=0}^{r_0} P_r(r)dr. \tag{15}$$

For the $w_0 = -1.0$, $w_a = -0.4$ cosmology of Figs. 5 and 6, the severity is $S = 0.29 \pm 0.09$. This model does not suffer a coincidence problem since 29% of observers would see r lower than we do. If the severity of the cosmic coincidence would be near 0.95 (0.997) in a particular model, then that model would suffer a 2σ (3σ) coincidence problem and the value of r we observe really would be unexpectedly high.

We calculated the severities S for cosmologies spanning a large region of the $w_0 - w_a$ plane and show our results in Fig. 7 using contours of equal S. The severity of the coincidence problem is low (e.g. $S \lesssim 0.7$) for most combinations of w_0 and w_a shown. There is a coincidence problem, where the severity is high ($S \gtrsim 0.8$), in two regions of this parameter space. These are indicated in Fig. 7.

Some features in Fig. 7 are worth noting:

- Dominating the left of the plot, the severity of the coincidence increases towards the bottom left-hand corner. This is because as w_0 and w_a become more negative, the r peak becomes narrower, and is observed by fewer observers.

- There is a strong vertical dipole of coincidence severity centered at $(w_0 = 0, w_a = 0)$. For ($w_0 \approx$

$0, w_a > 0$) there is a large coincidence problem because in such models we would be currently witnessing the very closest approach between DE and matter, with $\rho_{de} \gg \rho_m$ for all earlier and later times (see Fig. 8c). For ($w_0 \approx 0, w_a < 0$) there is an anti-coincidence problem because in those models we would be currently witnessing the DDE's furthest excursion from the matter density, with ρ_{de} and ρ_m in closer proximity for all relevant earlier and later times, i.e., all times when $P_t(t)$ is non-negligible.

- There is a discontinuity in the contours running along $w_a = 0$ for phantom models ($w_0 < -1$). The distribution $P_t(t)$ is truncated by big-rip singularities in strongly phantom models (provided they remain phantom; $w_a > 0$). This truncation of late-time observers means that early observers who witness large values of r represent a greater fraction of the total population.

To illustrate these features, Fig. 8 shows the density histories and observer distributions for four specific examples selected from the $w_0 - w_a$ plane of Fig. 7.

We find that *all* observationally allowed combinations of w_0 and w_a result in low severities ($S < 0.4$), i.e., there are large ($> 60\%$) probabilities of observing the matter and vacuum density to be at least as close to each other as we observe them to be.

VI. DISCUSSION

It was not clear what DDE dynamics were required to solve the coincidence problem. Our analysis might have resulted in new constraints on the values of w_0 and w_a, by simply demanding that we do not live during a special time in which $r \sim 1$. There are regions of $w_0 - w_a$ parameter space that can be ruled out in this manner (see Fig. 7) however those points are already strongly excluded by observational constraints on w_0 and w_a. Therefore, the cosmic coincidence problem can not be used as a tool to further constrain DDE since the problem is solved for all DDE models satisfying observational constraints on w_0 and w_a.

The main result of our analysis is that any DDE model in agreement with current cosmological constraints has $\rho_{de} \sim \rho_m$ for a significant fraction of observers.

Interacting quintessence models in which the proximity parameter asymptotes to a constant at late times [18, 22, 26, 29, 30, 31, 33, 35, 38, 39, 40, 56] have been proposed as a solution to the coincidence problem. More recently, del Campo et al. [28, 34] have argued for a broader class of interacting quintessence models that "soften" the coincidence problem by predicting a very slowly varying (though not constant) proximity parameter. Our analysis finds that r need not asymptote to a constant, nor evolve particularly slowly, partially undermining the motivations for these interacting quintessence models.

Caldwell et al. [60] and Scherrer [32] have proposed that the coincidence problem may be solved by phantom models in which there is a future big-rip singularity because such cosmologies spend a significant fraction of their lifetimes in $r \sim 1$ states. In our work $P_t(t)$ is terminated by big-rip singularities in ripping models. In non-ripping models, however, the distribution is effectively terminated by the declining star formation rate. Therefore the big-rip gives phantom models only a marginal advantage over other models. This marginal advantage manifests as the discontinuity along $w_a = 0$ on the left side of Fig. 7.

We could improve our analysis, in the sense of getting tighter coincidence constraints (larger severities), if we used a less conservative $P_{\Delta t_{obs}}$. We used the most conservative choice - a delta function - because the present understanding of the time it takes to evolve into observers is too poorly developed to motivate any other form of $P_{\Delta t_{obs}}$. Another possible improvement is the DE equation of state parameterization. We used the current standard, $w = w_0 + w_a(1 - a)$, which may not parameterize some models well for very small or very large values of a.

We conclude that DDE models need not be fitted with exact tracking or oscillatory behaviors specifically to solve the coincidence by generating long or repeated periods of $\rho_{de} \sim \rho_m$. Also, interactions proposed to cause $\rho_{de} \sim \rho_m$ for long periods are not well motivated. Moreover phantom models have no significant advantage over other DDE models with respect to the coincidence problem discussed here.

ACKNOWLEDGMENTS

CE acknowledges a UNSW School of Physics postgraduate fellowship. CE thanks the ANU's RSAA for its kind hospitality, where this research was carried out.

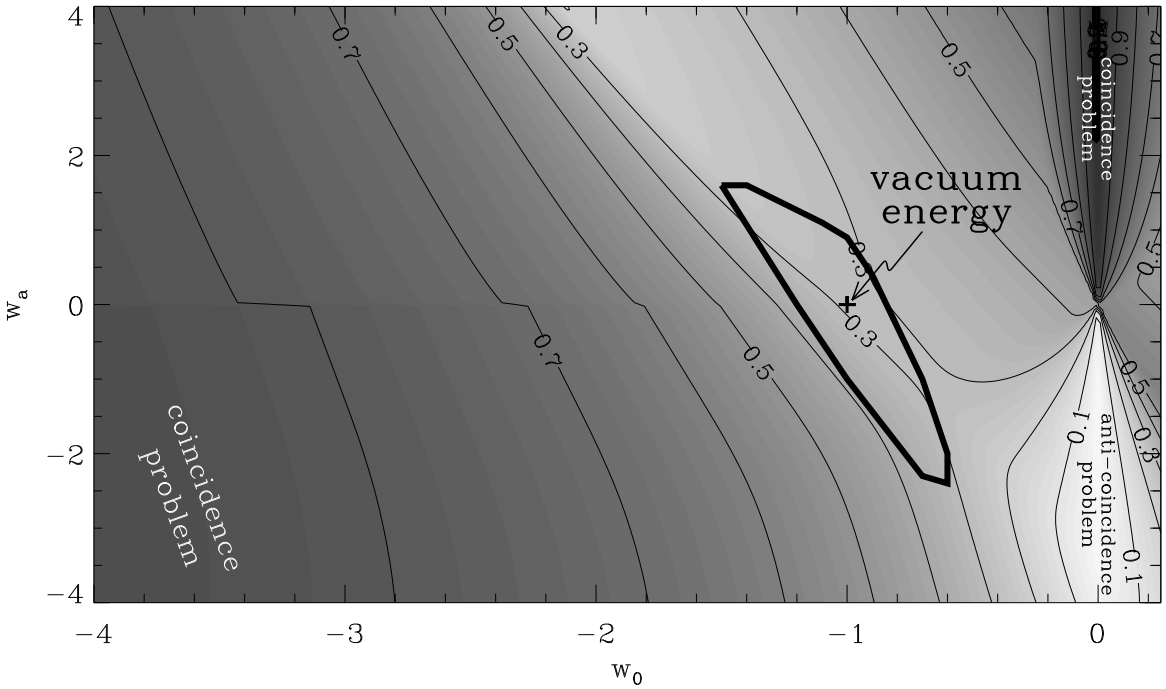

FIG. 7: Here we plot contours of equal severity S in $w_0 - w_a$ parameter space. S is the fraction of observers who see $r < r_0$. If S is large, a large percentage of observers should see r lower than we do - those models suffer coincidence problems. The thick black contour represents the observational constraints on w_0 and w_a from Davis et al. [67] (2σ confidence and marginalized over other uncertainties). In Lineweaver and Egan [12] we showed that the severity of the coincidence problem is low for ΛCDM (indicated by the "+"). Values of w_0 and w_a that result in a mild coincidence problem (e.g. $S \gtrsim 0.7$) are already strongly excluded by observations. This leads to our main result: none of the models in the observationally allowed regime suffer a cosmic coincidence problem when our estimate of the temporal distribution of observers $P_{obs}(t)$ is used as a selection function.

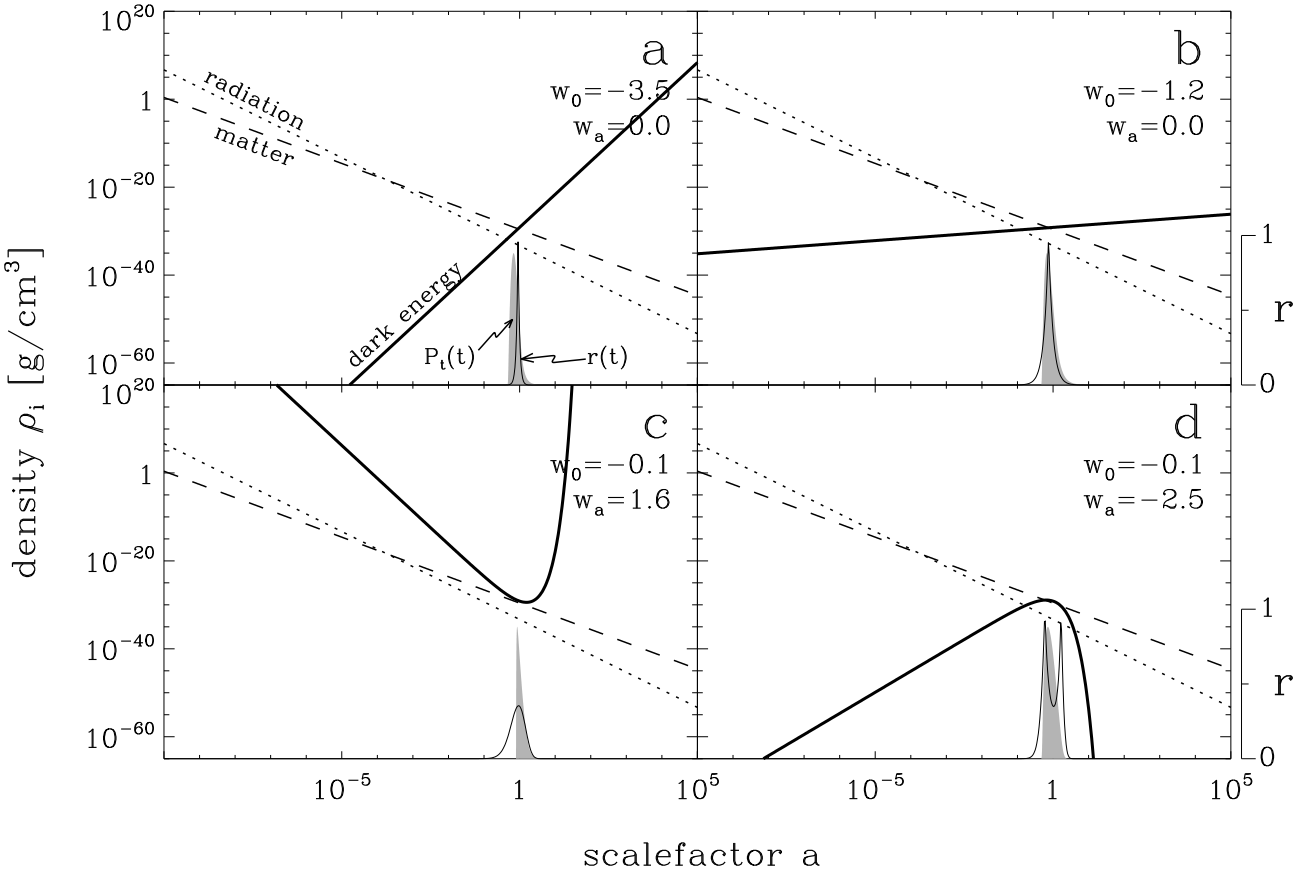

FIG. 8: History of the energy densities in radiation (dotted line), matter (dashed line) and dark energy (thick black line) for four parameterized DE models from Fig. 7. The proximity parameter r (thin black line) and the temporal distribution of observers $P_t(t)$ (grey shade) are also given. **Panel a** shows a phantom model with a constant equation of state $w = -3.5$. In this model the phantom density increases quickly and the $r(t)$ peak is narrow. As a result, a large fraction of observers live while the matter and dark energy densities are vastly different ($r \approx 0$) and there is a mild coincidence problem ($S \approx 0.8$). This might be used to rule-out the model shown in Panel a, except that it is already strongly excluded by direct cosmological observations (refer to Fig. 7). **Panel b** shows a phantom model which lies within the observationally allowed 2σ region. There is no coincidence problem in this model ($S \approx 0.4$). **Panel c** shows a model in which there is a coincidence problem ($S \approx 0.95$). This models lies within the cluster of contours in the upper right-hand corner of Fig. 7. In this model the dark energy dominates the past *and* future energy budget. Again however, the coincidence problem can tell us nothing new, as this model is already strongly excluded by observations. **Panel d** shows a model in which there is an anti-coincidence problem. This models lies within the cluster of contours in the lower right-hand corner of Fig. 7. In this model the dark energy and matter densities are more similar (r is greater) in the recent past and near future (although $r \to 0$ further into the past or future). According to the observer distribution $P_t(t)$ most observers live near the current epoch, during $r > 0.35$, with just 7% living during $r < 0.35$ ($S = 0.07$) in this particular model. One might argue that this model can be ruled out because our value of r is anomalously small. However, this model too is already strongly excluded by observations.

APPENDIX A: NUMERICAL VALUES FOR PARAMETERS OF MODELS ILLUSTRATED IN FIG. 2

TABLE I: Free parameters of the DDE models illustrated in Fig. 2. These values were chosen such that observational constraints are crudely satisfied. These are by no means the only combinations fitting observations. These values are intended for the purposes of illustration in Fig. 2. Units are Planck units.

Model	Parameter	Value
power law tracker quintessence	α	2
	M	1.4×10^{-124}
exponential tracker quintessence	M	1.3×10^{-124}
tracking oscillating energy	M	1.8×10^{-126}
	λ	4
	A	0.99
	ν	2.7
interacting quintessence	A	1.4×10^{-119}
	B	9.7
	C	16
Chaplygin gas	α	1
	A	2.8×10^{-246}

[1] A. G. Riess, A. V. Filippenko, P. Challis, A. Clocchiatti, A. Diercks, P. M. Garnavich, R. L. Gilliland, C. J. Hogan, S. Jha, R. P. Kirshner, et al., AJ **116**, 1009 (1998), arXiv:astro-ph/9805201.

[2] S. Perlmutter, G. Aldering, G. Goldhaber, R. A. Knop, P. Nugent, P. G. Castro, S. Deustua, S. Fabbro, A. Goobar, D. E. Groom, et al., ApJ **517**, 565 (1999), arXiv:astro-ph/9812133.

[3] C. H. Lineweaver, ApJ **505**, L69 (1998), arXiv:astro-ph/9805326.

[4] Y. B. Zel'Dovich, Soviet Journal of Experimental and Theoretical Physics Letters **6**, 316 (1967).

[5] R. Durrer and R. Maartens, ArXiv e-prints **711** (2007), 0711.0077.

[6] G. Hinshaw, *Legacy Archive for Microwave Background Data Analaysis (LAMBDA)*, Online Archive: http://lambda.gsfc.nasa.gov/product/map/current/params/lcdm_wmap_sdss.cfm (2006).

[7] S. Weinberg, Reviews of Modern Physics **61**, 1 (1989).

[8] J. D. Cohn, Ap&SS **259**, 213 (1998), arXiv:astro-ph/9807128.

[9] S. Weinberg, ArXiv Astrophysics e-prints (2000), astro-ph/0005265.

[10] P. J. Steinhardt, Royal Society of London Philosophical Transactions Series A **361**, 2497 (2003).

[11] S. M. Carroll, SNAP (SuperNova Acceleration Probe) Yellow Book astro-ph/0107571 (2001), astro-ph/0107571.

[12] C. H. Lineweaver and C. A. Egan, ArXiv Astrophysics e-prints (2007), astro-ph/0703429.

[13] G. Efstathiou, MNRAS **274**, L73 (1995).

[14] H. Martel, P. R. Shapiro, and S. Weinberg, ApJ **492**, 29 (1998), astro-ph/9701099.

[15] J. Garriga, M. Livio, and A. Vilenkin, Phys. Rev. D **61**, 023503 (1999), astro-ph/9906210.

[16] S. Weinberg, Physical Review Letters **59**, 2607 (1987).

[17] L. Pogosian and A. Vilenkin, Journal of Cosmology and Astro-Particle Physics **1**, 25 (2007), astro-ph/0611573.

[18] L. Amendola, Phys. Rev. D **62**, 043511 (2000), arXiv:astro-ph/9908023.

[19] S. Dodelson, M. Kaplinghat, and E. Stewart, Physical Review Letters **85**, 5276 (2000), astro-ph/0002360.

[20] V. Sahni and L. Wang, Phys. Rev. D **62**, 103517 (2000), arXiv:astro-ph/9910097.

[21] L. P. Chimento, A. S. Jakubi, and D. Pavón, Phys. Rev. D **62**, 063508 (2000), arXiv:astro-ph/0005070.

[22] W. Zimdahl, D. Pavón, and L. P. Chimento, Physics Letters B **521**, 133 (2001), arXiv:astro-ph/0105479.

[23] V. Sahni, Classical and Quantum Gravity **19**, 3435 (2002), arXiv:astro-ph/0202076.

[24] L. P. Chimento, A. S. Jakubi, and D. Pavón, Phys. Rev. D **67**, 087302 (2003), arXiv:astro-ph/0303160.

[25] M. Ahmed, S. Dodelson, P. B. Greene, and R. Sorkin, Phys. Rev. D **69**, 103523 (2004), astro-ph/0209274.

[26] U. França and R. Rosenfeld, Phys. Rev. D **69**, 063517 (2004), arXiv:astro-ph/0308149.

[27] M. R. Mbonye, Modern Physics Letters A **19**, 117 (2004), arXiv:astro-ph/0212280.

[28] S. del Campo, R. Herrera, and D. Pavón, Phys. Rev. D **71**, 123529 (2005), arXiv:astro-ph/0506482.

[29] Z.-K. Guo and Y.-Z. Zhang, Phys. Rev. D **71**, 023501 (2005), astro-ph/0411524.

[30] G. Olivares, F. Atrio-Barandela, and D. Pavón, Phys. Rev. D **71**, 063523 (2005), arXiv:astro-ph/0503242.

[31] D. Pavón and W. Zimdahl, Physics Letters B **628**, 206 (2005), arXiv:gr-qc/0505020.

[32] R. J. Scherrer, Phys. Rev. D **71**, 063519 (2005), arXiv:astro-ph/0410508.

[33] X. Zhang, Modern Physics Letters A **20**, 2575 (2005), arXiv:astro-ph/0503072.

[34] S. del Campo, R. Herrera, G. Olivares, and D. Pavón, Phys. Rev. D **74**, 023501 (2006), arXiv:astro-ph/0606520.

[35] U. França, Physics Letters B **641**, 351 (2006), arXiv:astro-ph/0509177.

[36] B. Feng, M. Li, Y.-S. Piao, and X. Zhang, Physics Letters B **634**, 101 (2006), astro-ph/0407432.

[37] S. Nojiri and S. D. Odintsov, Physics Letters B **637**, 139 (2006), arXiv:hep-th/0603062.

[38] L. Amendola, M. Quartin, S. Tsujikawa, and I. Waga, Phys. Rev. D **74**, 023525 (2006), arXiv:astro-ph/0605488.

[39] L. Amendola, G. C. Campos, and R. Rosenfeld, Phys. Rev. D **75**, 083506 (2007), arXiv:astro-ph/0610806.

[40] G. Olivares, F. Atrio-Barandela, and D. Pavon, ArXiv e-prints **706** (2007), 0706.3860.

[41] G. Sassi and S. A. Bonometto, New Astronomy **12**, 353 (2007), arXiv:astro-ph/0609568.

[42] A. Hebecker and C. Wetterich, Physics Letters B **497**, 281 (2001), arXiv:hep-ph/0008205.

[43] S. Bludman, Phys. Rev. D **69**, 122002 (2004), astro-ph/0403526.

[44] E. V. Linder, Phys. Rev. D **73**, 063010 (2006), arXiv:astro-ph/0601052.

[45] E. J. Copeland, M. Sami, and S. Tsujikawa, ArXiv High Energy Physics - Theory e-prints (2006), hep-th/0603057.

[46] M. Szydłowski, A. Kurek, and A. Krawiec, Physics Letters B **642**, 171 (2006), arXiv:astro-ph/0604327.

[47] M. Özer and M. O. Taha, Nuclear Physics B **287**, 776 (1987).

[48] B. Ratra and P. J. E. Peebles, Phys. Rev. D **37**, 3406 (1988).

[49] P. G. Ferreira and M. Joyce, Phys. Rev. D **58**, 023503 (1998), astro-ph/9711102.

[50] R. R. Caldwell, R. Dave, and P. J. Steinhardt, Physical Review Letters **80**, 1582 (1998), astro-ph/9708069.

[51] P. J. Steinhardt, L. Wang, and I. Zlatev, Phys. Rev. D **59**, 123504 (1999), astro-ph/9812313.

[52] I. Zlatev, L. Wang, and P. J. Steinhardt, Physical Review Letters **82**, 896 (1999), astro-ph/9807002.

[53] N. Dalal, K. Abazajian, E. Jenkins, and A. V. Manohar, Physical Review Letters **87**, 141302 (2001), astro-ph/0105317.

[54] G. Yang and A. Wang, General Relativity and Gravitation **37**, 2201 (2005), arXiv:astro-ph/0510006.

[55] L. Amendola, MNRAS **312**, 521 (2000), arXiv:astro-ph/9906073.

[56] L. Amendola and C. Quercellini, Phys. Rev. D **68**, 023514 (2003), arXiv:astro-ph/0303228.

[57] A. G. Riess, L.-G. Strolger, J. Tonry, S. Casertano, H. C. Ferguson, B. Mobasher, P. Challis, A. V. Filippenko, S. Jha, W. Li, et al., ApJ **607**, 665 (2004), arXiv:astro-ph/0402512.

[58] W. M. Wood-Vasey, G. Miknaitis, C. W. Stubbs, S. Jha, A. G. Riess, P. M. Garnavich, R. P. Kirshner, C. Aguilera, A. C. Becker, J. W. Blackman, et al., ArXiv Astrophysics e-prints (2007), astro-ph/0701041.

[59] R. R. Caldwell, Physics Letters B **545**, 23 (2002), arXiv:astro-ph/9908168.

[60] R. R. Caldwell, M. Kamionkowski, and N. N. Weinberg, Physical Review Letters **91**, 071301 (2003), arXiv:astro-ph/0302506.

[61] T. Chiba, T. Okabe, and M. Yamaguchi, Phys. Rev. D **62**, 023511 (2000), arXiv:astro-ph/9912463.

[62] C. Armendariz-Picon, V. Mukhanov, and P. J. Steinhardt, Physical Review Letters **85**, 4438 (2000), astro-ph/0004134.

[63] C. Armendariz-Picon, V. Mukhanov, and P. J. Steinhardt, Phys. Rev. D **63**, 103510 (2001), arXiv:astro-ph/0006373.

[64] M. Malquarti, E. J. Copeland, and A. R. Liddle, Phys. Rev. D **68**, 023512 (2003), arXiv:astro-ph/0304277.

[65] M. C. Bento, O. Bertolami, and A. A. Sen, Phys. Rev. D **66**, 043507 (2002), arXiv:gr-qc/0202064.

[66] A. Kamenshchik, U. Moschella, and V. Pasquier, Physics Letters B **511**, 265 (2001), gr-qc/0103004.

[67] T. M. Davis, E. Mortsell, J. Sollerman, A. C. Becker, S. Blondin, P. Challis, A. Clocchiatti, A. V. Filippenko, R. J. Foley, P. M. Garnavich, et al., ArXiv Astrophysics e-prints (2007), astro-ph/0701510.

[68] A. G. Riess, L.-G. Strolger, S. Casertano, H. C. Ferguson, B. Mobasher, B. Gold, P. J. Challis, A. V. Filippenko, S. Jha, W. Li, et al., ApJ **659**, 98 (2007), arXiv:astro-ph/0611572.

[69] Y. Wang and M. Tegmark, Phys. Rev. D **71**, 103513 (2005), arXiv:astro-ph/0501351.

[70] Y. Wang and P. Mukherjee, ApJ **650**, 1 (2006), arXiv:astro-ph/0604051.

[71] G. Efstathiou and J. R. Bond, MNRAS **304**, 75 (1999), arXiv:astro-ph/9807103.

[72] O. Elgarøy and T. Multamäki, A&A **471**, 65 (2007), arXiv:astro-ph/0702343.

[73] D. N. Spergel, R. Bean, O. Dore', M. R. Nolta, C. L. Bennett, G. Hinshaw, N. Jarosik, E. Komatsu, L. Page, H. V. Peiris, et al., astro-ph/0603449 http://lambda.gsfc.nasa.gov/product/map/dr2/params/lcdm-all.cfm (2006), astro-ph/0603449.

[74] D. J. Eisenstein and W. Hu, ApJ **496**, 605 (1998), arXiv:astro-ph/9709112.

[75] D. J. Eisenstein, I. Zehavi, D. W. Hogg, R. Scoccimarro, M. R. Blanton, R. C. Nichol, R. Scranton, H.-J. Seo, M. Tegmark, Z. Zheng, et al., ApJ **633**, 560 (2005), arXiv:astro-ph/0501171.

[76] K. Glazebrook, C. Blake, W. Couch, D. Forbes, M. Drinkwater, R. Jurek, K. Pimbblet, B. Madore, C. Martin, T. Small, et al., ArXiv Astrophysics e-prints (2007), astro-ph/0701876.

[77] B. M. S. Hansen, H. B. Richer, G. G. Fahlman, P. B. Stetson, J. Brewer, T. Currie, B. K. Gibson, R. Ibata,

R. M. Rich, and M. M. Shara, ApJS **155**, 551 (2004), arXiv:astro-ph/0401443.

[78] C. H. Lineweaver, Science **284**, 1503 (1999), astro-ph/9911493.

[79] R. Bean, S. H. Hansen, and A. Melchiorri, Phys. Rev. D **64**, 103508 (2001), arXiv:astro-ph/0104162.

[80] E. di Pietro and J.-F. Claeskens, MNRAS **341**, 1299 (2003), arXiv:astro-ph/0207332.

[81] A. Albrecht, G. Bernstein, R. Cahn, W. L. Freedman, J. Hewitt, W. Hu, J. Huth, M. Kamionkowski, E. W. Kolb, L. Knox, et al., ArXiv Astrophysics e-prints (2006), astro-ph/0609591.

[82] E. V. Linder, Astroparticle Physics **26**, 102 (2006), arXiv:astro-ph/0604280.

[83] E. V. Linder and D. Huterer, Phys. Rev. D **72**, 043509 (2005), arXiv:astro-ph/0505330.

[84] Y. Wang and M. Tegmark, Physical Review Letters **92**, 241302 (2004), arXiv:astro-ph/0403292.

[85] D. Huterer and A. Cooray, Phys. Rev. D **71**, 023506 (2005), arXiv:astro-ph/0404062.

[86] S. M. Carroll, *Spacetime and geometry. An introduction to general relativity* (Spacetime and geometry / Sean Carroll. San Francisco, CA, USA: Addison Wesley, ISBN 0-8053-8732-3, 2004, XIV + 513 pp., 2004).

[87] B. Carter, in *IAU Symp. 63: Confrontation of Cosmological Theories with Observational Data*, edited by M. S. Longair (1974), pp. 291–298.

[88] R. H. Dicke, Nature **192**, 440 (1961).

[89] A. Vilenkin, Physical Review Letters **74**, 846 (1995), gr-qc/9406010.

[90] B. E. J. Pagel, *Nucleosynthesis and Chemical Evolution of Galaxies* (Nucleosynthesis and Chemical Evolution of Galaxies, by Bernard E. J. Pagel, pp. 392. ISBN 0521550610. Cambridge, UK: Cambridge University Press, October 1997., 1997).

[91] C. H. Lineweaver and D. Grether, ApJ **598**, 1350 (2003), astro-ph/0306524.

[92] C. H. Lineweaver, Icarus **151**, 307 (2001), astro-ph/0012399.